Article

Optimization of Activity-Based Probes for Proteomic Profiling of Histone Deacetylase Complexes

Cleo M. Salisbury, and Benjamin F. Cravatt

J. Am. Chem. Soc., **2008**, 130 (7), 2184-2194 • DOI: 10.1021/ja074138u

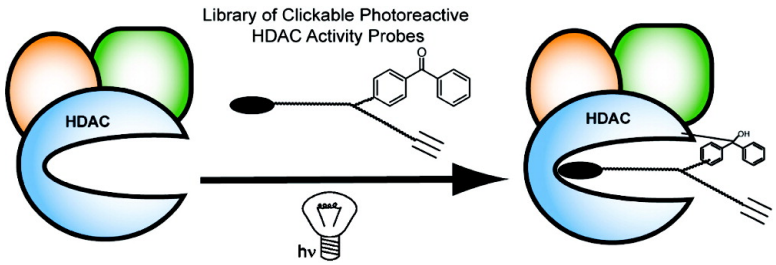

More About This Article

Additional resources and features associated with this article are available within the HTML version:

- Supporting Information
- Links to the 4 articles that cite this article, as of the time of this article download
- Access to high resolution figures
- Links to articles and content related to this article
- Copyright permission to reproduce figures and/or text from this article

View the Full Text HTML

J|A|C|S
ARTICLES
Published on Web 01/25/2008

Optimization of Activity-Based Probes for Proteomic Profiling of Histone Deacetylase Complexes

Cleo M. Salisbury and Benjamin F. Cravatt*

The Skaggs Institute for Chemical Biology and Department of Chemical Physiology, The Scripps Research Institute, 10550 North Torrey Pines Road, La Jolla, California 92037

Received June 6, 2007; E-mail: cravatt@scripps.edu

Abstract: Histone deacetylases (HDACs) are key enzymatic regulators of the epigenome and serve as promising targets for anticancer therapeutics. Recently, we developed a photoreactive "clickable" probe, SAHA-BPyne, to report on HDAC activity and complex formation in native biological systems. Here, we investigate the selectivity, sensitivity, and inhibitory properties of SAHA-BPyne and related potential activity-based probes for HDACs. While we identified several probes that are potent HDAC inhibitors and label HDAC complex components in native proteomic preparations, SAHA-BPyne was markedly superior for profiling HDAC activities in live cells. Interestingly, the enhanced performance of SAHA-BPyne as an *in situ* activity-based probe could not be solely ascribed to potency in HDAC binding, implying that other features of the molecule were key to efficient active site-directed labeling in living systems. Finally, we demonstrate the value of *in situ* profiling of HDACs by comparing the activity and expression of HDAC1 in cancer cells treated with the cytotoxic agent parthenolide. These results underscore the utility of activity-based protein profiling for studying HDAC function and may provide insight for the future development of click chemistry-based photoreactive probes for the *in situ* anaylsis of additional enzyme activities.

Introduction

The human genome encodes ~20 histone deacetylases (HDACs), a family of hydrolytic enzymes that catalyze the removal of acetyl groups from the side chain of lysines found in histone (and other) proteins. Since the downstream effects of histone acetylation include changes to chromatin conformation, an increase in apoptosis and differentiation, and a decrease in cell growth, there is a growing interest in the development of HDAC inhibitors as anticancer agents.[1−3] A number of small molecule HDAC inhibitors have been reported (Figure 1), some of which induce differentiation in cancer cell lines and reduce tumor volume *in vivo*.[1−3] Recently, suberoylanilide hydroxamic acid (SAHA, Vorinostat, **1**, Figure 1) was approved by the FDA for the treatment of cutaneous T cell lymphoma, and several other HDAC inhibitors are in clinical development.[1−3]

Despite the intense pursuit of HDAC-targeted therapeutics, we do not yet fully understand the connection between HDACs and cancer on a molecular level. Many of the HDAC inhibitors in clinical development, including SAHA, target several of the 11 known metal-dependent (formally Zn^{2+}-dependent) HDACs in humans. Efforts to rigorously understand which HDACs are critical for cancer pathogenesis are complicated by the fact that most of these enzymes are found in a variety of large multisubunit complexes that regulate both HDAC activity and substrate specificity.[4−6] Studies are further confounded by difficulties in reconstituting HDAC activities in purified, recombinant systems.[3,7] New methods are thus needed to monitor the functional state of HDAC complexes in native biological systems. Recently, we developed an active-site directed chemical probe, SAHA-BPyne (**5**, Figure 2), for profiling HDAC activities in proteomes and live cells.[8]

The previously reported SAHA-BPyne was designed based on the scaffold of SAHA, a reversible HDAC inhibitor with a hydroxamic acid moiety that chelates to the metal cation in HDAC active sites to provide high nanomolar to low micromolar inhibition.[2] To convert SAHA into an irreversible probe compatible with activity-based protein profiling (ABPP)[9,10] experiments, we introduced a benzophenone group into SAHA-BPyne, which can be photoactivated to promote covalent labeling of proximal proteins. We also appended an alkyne moiety onto SAHA-BPyne to facilitate click chemistry-mediated conjugation of reporter tags for the rapid and sensitive detection and affinity enrichment of probe-labeled proteins.[11,12] Here, we investigate in more detail the proteome labeling profiles and

(1) Marks, P. A.; Breslow, R. *Nat. Biotechnol.* **2007**, *25*, 84−90.
(2) Bolden, J. E.; Peart, M. J.; Johnstone, R. W. *Nat. Rev. Drug Discovery* **2006**, *5*, 769−84.
(3) Dokmanovic, M.; Clarke, C.; Marks, P. A. *Mol. Cancer Res.* **2007**, *5*, 981−89.
(4) You, A.; Tong, J. K.; Grozinger, C. M.; Schreiber, S. L. *Proc. Natl. Acad. Sci. U.S.A.* **2001**, *98*, 1454−8.
(5) Zhang, Y.; Ng, H. H.; Erdjument-Bromage, H.; Tempst, P.; Bird, A.; Reinberg, D. *Genes Dev.* **1999**, *13*, 1924−35.
(6) Pflum, M. K.; Tong, J. K.; Lane, W. S.; Schreiber, S. L. *J. Biol. Chem.* **2001**, *276*, 47733−41.
(7) Curtin, M.; Glaser, K. *Curr. Med. Chem.* **2003**, *10*, 2373−92.
(8) Salisbury, C. M.; Cravatt, B. F. *Proc. Natl. Acad. Sci. U.S.A.* **2007**, *104*, 1171−6.
(9) Evans, M. J.; Cravatt, B. F. *Chem. Rev.* **2006**, *106*, 3279−301.
(10) Jessani, N.; Cravatt, B. F. *Curr. Opin. Chem. Biol.* **2004**, *8*, 54−9.
(11) Speers, A. E.; Adam, G. C.; Cravatt, B. F. *J. Am. Chem. Soc.* **2003**, *125*, 4686−7.
(12) Speers, A. E.; Cravatt, B. F. *Chem. Biol.* **2004**, *11*, 535−46.

10.1021/ja074138u CCC: $40.75

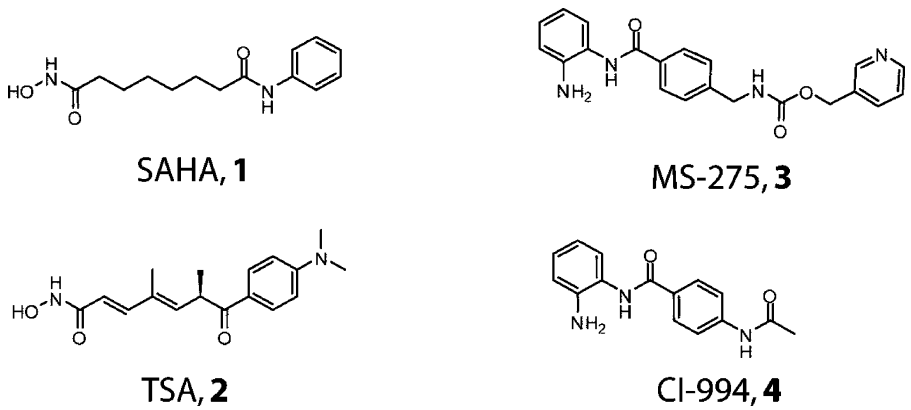

Figure 1. Structures of representative HDAC inhibitors.

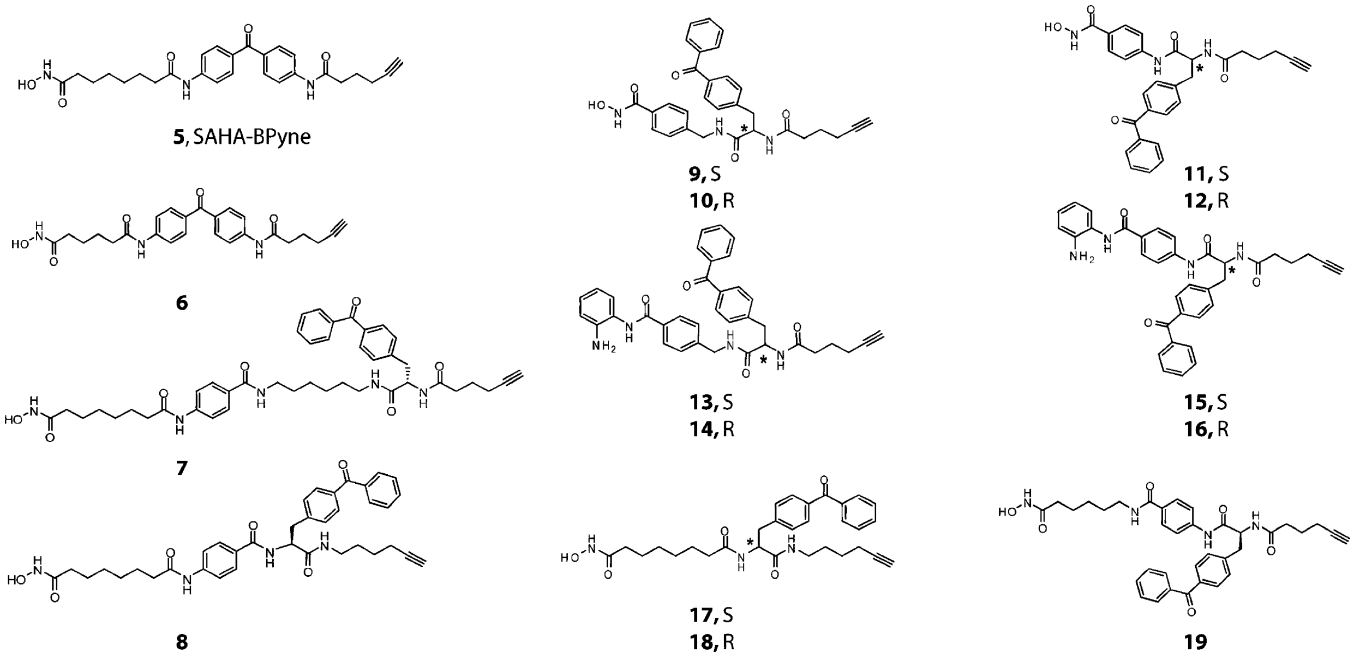

Figure 2. Structures of candidate ABPP probes for HDACs. Stereochemistry of benzophenone amino acid in compounds **9**−**18** (asterisks) is noted next to the compound numbers.

inhibitory properties of SAHA-BPyne and demonstrate that this probe has a rare ability, relative to closely related analogues, to label HDACs in living cells. Furthermore, we demonstrate that SAHA-BPyne, and more generally, the ABPP technology, provides a unique perspective for understanding the interplay between enzyme abundance and enzyme activity in living cells.

Experimental Section

Chemicals. Tris(2-carboxyethyl) phosphine (TCEP) was purchased from Fluka (St. Louis, MO). The click-chemistry ligand, tris[(1-benzyl-1*H*-1,2,3-triazol-4-yl)methyl]amine ("ligand"), was purchased from Aldrich (St. Louis, MO). Parthenolide was purchased from Tocris (Ellisville, MO). Resins, amino acids, and reagents for solid-phase peptide synthesis were purchased from EMD Biosciences (San Diego, CA) and Bachem (Torrance CA). SAHA (**1**)[8], SAHA-BPyne (**5**)[8], and rhodamine-azide[11] were prepared as described.

Cell Culture. The human uveal melanoma cell line MUM-2B (provided by Mary Hendrix at Northwestern University) was grown in RPMI medium 1640 containing 10% FCS. HCT-15 colon cancer cells and MDA-MB-231 breast cancer cells (both from the American Type Culture Collection) were grown in Advanced RPMI and DMEM media, respectively, with 10% FCS. Whole cell lysate was prepared by sonicating cell pellets in PBS. Soluble fractions were prepared by sonicating and Dounce homogenizing cell pellets in PBS, followed by centrifugation at 100 000 × *g* (45 min) to provide soluble cellular proteome fractions (supernatant) and a membrane pellet. Nuclear fractions were prepared by first adding cold 10 mM HEPES pH 7.7, 10 mM KCl, 0.1 mM EDTA, and 0.4% IGEPAL CA-630 to plates of washed cells. After 10 min at rt, the lysed cells were centrifuged at 15 000 × *g* for 3 min and the soluble fractions removed. The pellet was resuspended in 20 mM HEPES pH 7.7, 0.4 M NaCl, 10% glycerol by vortexing for 2 h at 4 °C, followed by centrifugation at 15 000 × *g* (5 min, 4 °C) to provide the nuclear fractions (supernatant) and a membrane pellet. All fractions were stored at −80 °C until use.

***In Vitro* Proteome Labeling and Analysis.** Proteome samples were diluted in PBS to 50 μL at a final concentration of 1 mg/mL protein (4 mg/mL for whole cell lysate). SAHA-BPyne was added to samples at a final concentration of 50 nM−5 μM in the presence or absence of excess SAHA competitor (final concentration of 1 μM−50 μM). All samples were then placed into the wells of an ice-cooled 96-well plate and irradiated at 365 nm using a Spectroline ENF 260C UV lamp for 1 h on ice. After UV cross-linking, rhodamine-azide (12.5−100 μM final concentration) was added, followed by TCEP (0.5 mM final concentration) and ligand (100 μM final concentration). Samples were gently vortexed, and the cycloaddition was initiated by the addition of $CuSO_4$ (1 mM final concentration). The click chemistry reactions were

incubated at rt for 1 h. An equal volume of 2× standard SDS loading buffer was added, and the samples were separated by 1D SDS-PAGE and visualized by in-gel fluorescent scanning using a Hitachi FMBio Ile flatbed scanner (MiraiBio, Alameda CA).

***In Situ* Labeling of Cancer Cells.** MUM2B cells, grown to 90% confluency in 6 cm dishes, were washed with PBS (3 × 3 mL) and treated with 1 mL of PBS containing probe (50 nM−25 μM), with or without excess SAHA (10×). The samples were irradiated at 365 nm at 37 °C for 6 min (13 min for concentration gradient study) by placing a Spectroline ENF 260C UV approximately 1″ above the covered dish of cells. After irradiation, the cells were washed with PBS (3 × 3 mL), scraped, and pelleted by centrifugation. The cell pellet was resuspended in PBS (50 μL), homogenized by sonication, and diluted to 2.5 mg/mL with PBS (4 mg/mL for concentration gradient). To initiate the click chemistry reaction, rhodamine azide (100 μM final concentration), TCEP (0.5 mM final concentration), ligand (100 μM final concentration), and $CuSO_4$ (1 mM final concentration) were added. The reactions were incubated at rt for 1 h. An equal volume of 2× loading buffer was added, and the samples were separated by 1D SDS-PAGE and visualized and by in-gel fluorescent scanning.

Parthenolide-treated cells were grown to ∼70% confluency, and the media was replaced with media containing 15 μM parthenolide. After incubating the cells for 3 h at 37 °C, the cells were washed in cold PBS and treated with SAHA-BPyne (2 μM) with or without excess SAHA (40 μM) using the above conditions. After click chemistry, SDS-PAGE separation, and scanning as described above, labeled proteins were quantified by measuring the integrated band intensities.

Western Blotting. All samples were separated on SDS-PAGE gels and transferred to nitrocellulose. The blots were blocked with 3% milk in TBST, probed with polyclonal α-HDAC1 (1:800 in TBST, 06-720, Upstate, Lake Placid NY) for 2 h at rt, washed with TBST, incubated with goat-α-rabbit IgG (H + L) HRP conjugate (1:20000, Biorad, Hercules CA) for 2 h at rt, washed again in TBST, and visualized with a SuperSignal West Pico kit (Pierce, Rockford IL).

Alternate Probe Synthesis. Unless otherwise noted, chemicals were obtained from commercial suppliers and used without further purification. Dry THF and CH_2Cl_2 were obtained by passing commercially available predried, oxygen-free formulations through activated alumina columns. NMR spectra were obtained in DMSO-d_6 and were recorded on a Bruker DRX-500 instrument unless otherwise noted. NMR chemical shifts are reported in ppm downfield relative to the internal solvent peak, and J values are in Hz. High-resolution mass spectrometry data (HRMS) were performed at The Scripps Research Institute Mass Spectrometry Core and recorded on an Agilent mass spectrometer using ESI-TOF (electrospray ionization-time-of-flight). Preparatory HPLC was performed with a C18 column (Higgins Analytical, 5 μm, 150 mm × 10 mm) gradient of CH_3CN/H_2O−0.1% TFA, 5−66% over 50 min, 5 mL/min, with detection at 280 nm for 70 min. Analytical HPLC was performed with a C18 column (Higgins Analytical, 5 μm, 150 mm × 4.6 mm) gradient of CH_3CN/H_2O−0.1% TFA, 5−95% over 17 min, 0.5 mL/min, with detection at 220/254/280 nm for 22 min.

Probe 6 (CSIV.87). To a flame-dried 2 dram vial fitted with a stir bar were added *N*-(4-(4-aminobenzoyl)phenyl)hex-5-ynamide[8] (35 mg, 0.11 mmol), *i*-Pr_2EtN (38 μL, 0.22 mmol), and THF (700 μL). The flask was cooled to 0 °C in an ice bath, and methyl adipoyl chloride (24 μL, 0.14 mmol) was added. The mixture was allowed to warm to rt and stirred overnight. CH_2Cl_2 (5 mL) was added to the reaction, and the organic layer was washed with $NaHCO_3$ (sat., 5 mL) and 10% citric acid (5 mL). The organic layer was dried (Na_2SO_4) and filtered, and the solvent was removed by rotary evaporation to provide the methyl ester analogue of the probe as a yellow solid (32 mg, 65% yield, HR-MS m/z calcd for $C_{26}H_{28}N_2O_5$ (M + H): 449.2071. Found: 449.2052). To a 2 dram vial fitted with a stir bar were added the methyl ester intermediate (13 mg, 0.03 mmol), DMF (300 μL), THF (300 μL), and 50% H_2NOH in water (300 μL, 5 mmol). After stirring overnight, the THF was removed *in vacuo*, and the remainder of the sample was purified using preparatory C18 reversed-phase HPLC (t_R: 20.7 min) to afford 7.7 mg (58%) of probe **6** as a yellow solid. t_R (analytical): 13.2 min. ^{1}H NMR (500 MHz) δ 1.62−1.65 (m, 4H), 1.84 (quintet, J = 7.1, 2H), 2.04 (t, J = 6.7, 2H), 2.30 (td, J = 7.0, 2.5, 2H), 2.42 (t, J = 6.7, 2H), 2.53−2.56 (m, 2H), 2.89 (t, J = 2.6, 1H), 7.75−7.83 (m, 8H), 10.20−10.42 (m, 3H). ^{13}C NMR (125 MHz) δ 18.21, 24.65, 25.58, 27.70, 33.02, 36.07, 37.19, 72.57, 84.83, 119.05, 119.08, 131.75, 131.92, 132.55, 132.59, 143.88, 143.94, 172.09, 172.32, 172.58, 194.23. HR-MS m/z calcd for $C_{25}H_{27}N_3O_5$ (M + H): 450.2023. Found: 450.2011.

Probe 7 (CSIV.109). 4-(4-Formyl-3-methoxyphenoxy)butyryl (FMPB) AM resin (50 mg, 0.045 mmol) was added to a fritted syringe and swollen with dichloroethane (DCE, 1 mL). Monotrityl-protected 1,6-diaminohexane (188 mg, 0.450 mmol) in 2:1 DCE/trimethylorthoformate (TMOF) (0.5 mL) was added to the resin, followed by $NaBH(OAc)_3$ (85 mg, 0.45 mmol). The resin was agitated overnight and then successively washed with DMF, 10% *i*-Pr_2EtN in DMF, MeOH, THF, and DMF (1 × 1 mL each). A solution of Fmoc-4-benzoyl-L-phenylalanine (Fmoc-L-Bpa-OH, 108 mg, 0.220 mmol), *O*-(7-azabenzotriazol-1-yl)-1,1,3,3-tetramethyluroniumhexafluorophosphate (HATU, 84 mg, 0.22 mmol), and *i*-Pr_2EtN (74 μL, 0.45 mmol) in DMF (0.5 mL) was added to the resin and agitated for 4 h. The resin was then filtered and washed with DMF (3 × 1 mL), the Fmoc group was removed (subjected to 20% piperidine in DMF for 30 min), and the resin was washed again (3 × 1 mL DMF). A solution of hexynoic acid (24 μL, 0.22 mmol), HATU (84 mg, 0.22 mmol), and *i*-Pr_2EtN (74 μL, 0.45 mmol) in DMF (0.5 mL) was added to the resin and agitated for 4 h. The resin was then filtered and washed successively with DMF, THF, MeOH, THF, and CH_2Cl_2 (3 × 1 mL). The trityl group was removed by treatment with 2% TFA in CH_2Cl_2 (10 × 2 mL × 10 min), and the resin was washed with CH_2Cl_2 and DMF (3 × 1 mL). A solution of Fmoc-PABA-OH (79 mg, 0.22 mmol), HATU (84 mg, 0.22 mmol), and *i*-Pr_2EtN (74 μL, 0.45 mmol) in DMF (0.5 mL) was added to the resin and agitated for 4 h. The resin was then filtered and washed with DMF (3 × 1 mL), the Fmoc group was removed, and the resin was washed successively with DMF, THF, MeOH, THF, and CH_2Cl_2 (3 × 1 mL). A solution of methyl-8-chloro-8-oxooctanoate (51 μL, 0.36 mmol) and *i*-Pr_2EtN (60 μL, 0.36 mmol) in CH_2Cl_2 (0.5 mL) was added to the resin and agitated overnight. The acylation was repeated, and the resin was washed successively with DMF, THF, MeOH, THF, and CH_2Cl_2 (3 × 1 mL). The methyl ester analogue of the probe was cleaved from support by treatment with 97.5% TFA/2.5% H_2O (1 mL), and the eluant was concentrated by rotary evaporation. DMF (300 μL), THF (300 μL), and 50% H_2NOH in water (300 μL, 5 mmol) were added to the residue, and the reaction stirred for 48 h. The THF was removed *in vacuo*, and the remainder of the sample was purified using preparatory C18 reversed-phase HPLC to afford 2.1 mg (6%) of probe **7**. t_R (analytical): 14.2 min. ^{1}H NMR (500 MHz) δ 1.28−1.65 (m, 18H), 1.98−2.06 (m, 4H), 2.20 (td, J = 7.4, 1.7, 2H), 2.37 (t, J = 7.4, 2H), 2.60−2.62 (m, 1H), 2.78−2.80 (m, 1H), 2.89−2.95 (m, 2H), 3.06−3.14 (m, 3H), 3.27 (q, J = 6.7, 2H), 4.58−4.63 (m, 1H), 7.46 (d, J = 8.2, 2H), 7.61 (t, J = 7.7, 2H), 7.69−7.76 (m, 6H), 7.83 (d, J = 7.8, 2H), 8.02 (t, J = 5.5, 1H), 8.19 (d, J = 8.6, 1H), 8.33 (t, J = 5.6, 1H), 10.12 (s,1H), 10.38 (s, 1H). HR-MS m/z calcd for $C_{43}H_{53}N_5O_7$ (M + H): 752.4018. Found: 752.4005.

General Protocol for Preparation of Probes 8, 17, and 18. FMPB AM resin (50 mg, 0.045 mmol) was added to a fritted syringe and swollen with DCE (1 mL). 6-Aminohexyne hydrochloride[13] (61 mg, 0.45 mmol) in 2:1 DCE/TMOF (0.5 mL) was added to the resin, followed by $NaBH(OAc)_3$ (85 mg, 0.45 mmol). The resin was agitated overnight and then successively washed with DMF, 10% *i*-Pr_2EtN in DMF, MeOH, THF, and DMF (1 × 1 mL each). A solution of Fmoc-Bpa-OH (L for probes **8** and **18**, D for probe **17**, 108 mg, 0.220 mmol),

(13) Muller, T. E.; Lercher, J. A.; Van Nhu, N. *AIChE J.* **2003**, *49*, 214−24.

HATU (84 mg, 0.22 mmol), and *i*-Pr_2EtN (74 μL, 0.45 mmol) in DMF (0.5 mL) was added to the resin and agitated for 4 h. The resin was then filtered and washed with DMF (3 × 1 mL), the Fmoc group was removed (subjected to 20% piperidine in DMF for 30 min), and the resin was washed again (3 × 1 mL DMF). [For probe **8**, a solution of Fmoc-PABA-OH (79 mg, 0.22 mmol), HATU (84 mg, 0.22 mmol), and *i*-Pr_2EtN (74 μL, 0.45 mmol) in DMF (0.5 mL) was added to the resin and agitated for 4 h. The resin was then filtered and washed with DMF (3 × 1 mL), the Fmoc group was removed, and the resin was washed successively with DMF, THF, MeOH, THF, and CH_2Cl_2 (3 × 1 mL).] A solution of methyl-8-chloro-8-oxooctanoate (51 μL, 0.36 mmol) and *i*-Pr_2EtN (60 μL, 0.36 mmol) in CH_2Cl_2 (0.5 mL) was added to the resin and agitated overnight. The acylation was repeated, and the resin was washed successively with DMF, THF, MeOH, THF, and CH_2Cl_2 (3 × 1 mL). The methyl ester analogue of the probe was cleaved from support by treatment with 95% TFA/5% CH_2Cl_2 (1 mL), and the eluant was concentrated by rotary evaporation. DMF (300 μL), THF (300 μL), and 50% H_2NOH in water (300 μL, 5 mmol) were added to the residue, and the reaction stirred for 48 h. The THF was removed *in vacuo*, and the remainder of the sample was purified using preparatory C18 reversed-phase HPLC.

Probe 8 (CSIV104). The general procedure provided 4.7 mg (37%) of probe **8**. t_R(analytical): 14.8 min. ^{1}H NMR (500 MHz) δ 1.33−1.64 (m, 14H), 1.99 (t, J = 7.0, 2H), 2.20 (m, 2H), 2.37 (t, J = 7.4, 2H), 2.79 (m, 1H), 2.95 (m, 1H), 4.78 (m, 2H), 7.55−7.84 (m, 13H), 8.16 (br s,1H), 8.52 (br s,1H), 8.70 (br s,1H), 10.15 (s, 1H), 10.38 (s, 1H). HR-MS *m*/*z* calcd for $C_{37}H_{42}N_2O_6$ (M + H): 639.3177. Found: 639.3159.

Probe 17 (CSIV.108B). The general procedure provided 8.2 mg (36%) of probe **17**. t_R(analytical): 14.2 min. ^{1}H NMR (500 MHz) δ 1.15−1.24 (m, 4H), 1.40−1.52 (m, 8H), 1.95 (t, J = 7.4, 2H), 2.10 (t, J = 7.4, 2H), 2.19 (td, J = 6.9, 2.6, 2H), 2.78 (t, J = 2.7, 1H), 2.92 (dd, J = 9.4, 4.1, 1H), 3.07−3.15 (m, 3H), 4.58−4.61 (m, 1H), 7.47 (d, J = 8.2, 2H), 7.62 (t, J = 7.7, 2H), 7.70−7.76 (m, 5H), 8.04 (t, J = 5.6, 1H), 8.12 (d, J = 8.6, 1H), 10.36 (s, 1H). ^{13}C NMR (125 MHz) δ 18.24, 25.83, 25.95, 26.13, 28.99, 29.11, 29.20, 33.10, 35.99, 38.77, 38.85, 54.42, 72.10, 85.22, 129.40, 130.25, 130.30, 130.41, 133.39, 135.88, 138.16, 144.30, 169.94, 171.63, 172.85, 196.35. HR-MS *m*/*z* calcd for $C_{30}H_{37}N_3O_5$ (M + H): 520.2806. Found: 520.2800.

Probe 18 (CSIV.108A). The general procedure provided 5.9 mg (26%) of probe **18**. t_R(analytical): 14.1 min. ^{1}H NMR (500 MHz) δ 1.16−1.26 (m, 4H), 1.41−1.52 (m, 8H), 1.95 (t, J = 7.3, 2H), 2.10 (t, J = 7.3, 2H), 2.19 (td, J = 6.8, 2.6, 2H), 2.78 (t, J = 2.1, 1H), 2.92 (dd, J = 9.5, 3.9, 1H), 3.05−3.17 (m, 3H), 4.57−4.62 (m, 1H), 7.47 (d, J = 8.2, 2H), 7.62 (t, J = 7.7, 2H), 7.70−7.76 (m, 5H), 8.04 (t, J = 5.7, 1H), 8.12 (d, J = 8.6, 1H), 10.36 (s, 1H). ^{13}C NMR (125 MHz) δ 18.22, 25.81, 25.93, 26.10, 28.97, 29.09, 29.18, 33.08, 35.99, 38.75, 38.84, 54.40, 72.10, 85.20, 129.39, 130.24, 130.29, 130.40, 133.38, 135.87, 138.15, 144.30, 169.93, 171.62, 172.85, 196.34. HR-MS *m*/*z* calcd for $C_{30}H_{37}N_3O_5$ (M + H): 520.2806. Found: 520.2799.

General Protocol for Preparation of Probes 9−12. Wang resin (200 mg, 0.220 mmol) was modified to display a resin bound *O*-hydroxylamine prepared as previously described.[14] A portion of the resin (60 mg) was added to a fritted syringe and swollen with CH_2Cl_2 (1 mL) for 1 h. A solution of Fmoc-Amb-OH (97 mg, 0.26 mmol) (for probes **9** and **10**) or Fmoc-PABA-OH (79 mg, 0.22 mmol) (for probes **11** and **12**), HATU (99 mg, 0.26 mmol), and *i*-Pr_2EtN (86 μL, 0.52 mmol) in DMF (0.5 mL) was added to the resin and agitated for 4 h. The resin was then filtered and washed with DMF (3 × 1 mL), the Fmoc group was removed (subjected to 20% piperidine in DMF for 30 min), and the resin was washed again (3 × 1 mL DMF). A solution of Fmoc-Bpa-OH (162 mg, 0.33 mmol) (L for probes **9** and **11**, D for probes **10** and **12**), HATU (99 mg, 0.26 mmol), and *i*-Pr_2EtN (86 μL, 0.52 mmol) in DMF (0.5 mL) was added to the resin and agitated overnight. The resin was then filtered and washed with DMF (3 × 1 mL), the Fmoc group was removed, and the resin was washed again (3 × 1 mL DMF). A solution of 6-hexynoic acid (36 μL, 0.33 mmol), HATU (125 mg, 0.33 mmol), and *i*-Pr_2EtN (109 μL, 0.66 mmol) in DMF (0.5 mL) was added to the resin and agitated for 4 h. The acylation was repeated overnight, and the resin was then filtered and washed successively with DMF, THF, MeOH, THF, and CH_2Cl_2 (3 × 1 mL). The probes were cleaved from support by treatment with 97.5% TFA/2.5% H_2O, and the eluant was concentrated and then purified using preparatory C18 reversed-phase HPLC.

Probe 9 (CSIV.102A). The general procedure provided 4.1 mg (15%) of probe **9**. t_R(analytical): 13.8 min. ^{1}H NMR (500 MHz) δ 1.60−1.66 (m, 2H), 2.06 (td, J = 7.2, 2.6, 2H), 2.23 (td, J = 7.4, 3.3, 2H), 2.79 (t, J = 2.6, 1H), 2.94−2.98 (m, 1H), 3.19 (dd, J = 13.7, 5.2, 1H), 4.38 (d, J = 5.9, 2H), 4.67−4.72 (m, 1H), 7.31 (d, J = 8.2, 2H), 7.50 (d, J = 8.2, 2H), 7.61−7.64 (m, 2H), 7.71−7.77 (m, 7H), 8.29 (d, J = 8.4, 1H), 8.64 (t, J = 5.9, 1H). ^{13}C NMR (125 MHz) δ 18.10, 25.13, 34.93, 42.732, 54.58, 72.25, 84.95, 100.01, 127.71, 127.76, 128.56, 129.40, 129.41, 130.27, 130.30, 130.32, 130.47, 133.37, 135.95, 138.17, 171.98, 172.39, 196.36. HR-MS *m*/*z* calcd for $C_{30}H_{29}N_3O_5$ (M + H): 512.218. Found: 512.2172.

Probe 10 (CSIV.102B). The general procedure provided 4.2 mg (15%) of probe **10**. t_R(analytical): 13.8 min. ^{1}H NMR (400 MHz) δ 1.52−1.60 (m, 2H), 1.99 (td, J = 7.2, 2.4, 2H), 2.16 (td, J = 7.3, 2.0, 2H), 2.74 (t, J = 2.6, 1H), 2.89 (dd, 13.0, 10.2, 1H), 3.13 (m, 13.4, 4.8, 1H), 4.32 (d, J = 5.9, 2H), 4.60−4.66 (m, 1H), 7.24 (d, J = 8.1, 2H), 7.43 (d, J = 8.2, 2H), 7.56 (t, J = 7.5, 2H), 7.65−7.71 (m, 7H), 8.25 (d, J = 8.5, 1H), 8.64 (t, J = 5.7, 1H). ^{13}C NMR (100 MHz) δ 17.25, 24.28, 34.07, 41.87, 53.74, 71.44, 84.10, 100.01, 126.87, 126.88, 128.56, 129.43, 129.49, 129.64, 131.28, 132.54, 135.09, 137.30, 142.53, 143.47, 171.15, 171.54, 195.52. HR-MS *m*/*z* calcd for $C_{30}H_{29}N_3O_5$ (M + H): 512.218. Found: 512.2171.

Probe 11 (CSIV.93). The general procedure provided 6.6 mg (24%) of probe **11**. t_R(analytical): 14.3 min. ^{1}H NMR (500 MHz) δ 1.62−1.68 (m, 2H), 2.09 (td, J = 7.3, 2.6, 2H), 2.25 (td, J = 7.5, 2.1, 2H), 2.80 (q, J = 2.6, 1H), 3.04 (dd, J = 13.4, 9.9, 1H), 3.20−3.23 (dd, J = 13.5, 4.9, 1H), 4.80−4.85 (m, 1H), 7.54 (d, J = 8.2, 2H), 7.61 (t, J = 7.7, 2H), 7.70−7.80 (m, 1H), 8.44 (d, J = 8.2, 1H), 10.42 (s, 1H). ^{13}C NMR (125 MHz) δ 18.09, 25.12, 34.79, 38.49, 55.40, 72.26, 84.92, 119.51, 128.55, 129.39, 130.28, 130.31, 130.33, 130.43, 133.40, 136.07, 138.11, 142.13, 143.82, 171.34, 172.58, 196.37. HR-MS *m*/*z* calcd for $C_{29}H_{27}N_3O_5$ (M + H): 498.2023. Found: 498.2014.

Probe 12 (CSIV.94). The general procedure provided 4.8 mg (18%) of probe **12**. t_R(analytical): 14.3 min. ^{1}H NMR (400 MHz) δ 1.28 (quintet, J = 7.2, 2H), 2.02 (td, J = 7.2, 2.6, 2H), 2.25 (dd, J = 7.2, 6.0, 2H), 2.75 (t, J = 2.6, 1H), 2.96 (dd, J = 13.4, 10.0, 1H), 3.14 (dd, J = 13.8, 5.0, 1H), 4.73−4.78(m, 1H), 7.47−7.73 (m, 13H), 8.40 (d, J = 8.2, 1H), 10.38 (s, 1H). ^{13}C NMR (125 MHz) δ 18.10, 25.14, 34.81, 38.49, 55.41, 72.28, 84.94, 119.51, 128.58, 129.40, 130.29, 130.29,130.34, 130.44, 133.41, 136.08, 138.12, 142.16, 143.82, 171.34, 172.58, 196.38. HR-MS *m*/*z* calcd for $C_{29}H_{27}N_3O_5$ (M + H): 498.2023. Found: 498.2007.

General Protocol for Preparation of Probes 13−16. A solution of Fmoc-Amb-OH (31 mg, 0.084 mmol) (for probes **13** and **14**) or Fmoc-PABA-OH (30 mg, 0.08 mmol) (for probes **15** and **16**) and *i*-Pr_2-EtN (46 μL, 0.28 mmol) in dry CH_2Cl_2 (0.5 mL) was added to a fritted syringe containing 2-chlorotrityl resin (50 mg, 0.07 mmol). After 4 h, the resin was filtered, quenched by the addition of *i*-Pr_2EtN/MeOH/CH_2Cl_2 (1:2:17), and washed with CH_2Cl_2 and DMF (3 × 1 mL). The Fmoc group was removed (subjected to 20% piperidine in DMF for 30 min), and the resin was washed again (3 × 1 mL DMF). A solution of Fmoc-Bpa-OH (172 mg, 0.350 mmol) (L for probes **13** and **15**, D for probes **14** and **16**), HATU (133 mg, 0.350 mmol), and *i*-Pr_2EtN (116 μL, 0.700 mmol) in DMF (0.5 mL) was added to the resin and agitated overnight. The resin was then filtered and washed with DMF

(14) Floyd, C. D.; Lewis, C. N.; Patel, S. R.; Whittaker, M. *Tet. Lett.* **1996**, *37*, 8045−8.

(3 × 1 mL), the Fmoc group was removed, and the resin was washed again (3 × 1 mL DMF). A solution of hexynoic acid (39 μL, 0.35 mmol), HATU (133 mg, 0.350 mmol), and *i*-Pr_2EtN (116 μL, 0.700 mmol) in DMF (0.5 mL) was added to the resin and agitated for 4 h. The acylation was repeated overnight, and the resin was then filtered and washed successively with DMF, THF, MeOH, THF, and CH_2Cl_2 (3 × 1 mL). The probes were cleaved from support by treatment with 5% TFA/95% CH_2Cl_2 (1 mL), and the eluant was concentrated and then purified using preparatory C18 reversed-phase HPLC. 1-Hydroxybenzotriazole (HOBt, 15 mg, 0.080 mmol) and DMF/DCE (1:6, 700 μL) were added to the residue. After the residue dissolved, 1-ethyl-3-[3-dimethylaminopropyl]carbodiimide hydrochloride (EDC, 15 mg, 0.080 mmol) was added and the reaction stirred for 5 min. 1,2-Phenylenediamine (76 mg, 0.70 mmol) was added to the reaction vessel, and the reaction stirred overnight. Additional portions of HOBt, EDC, and diamine were added to the reaction, and again the reaction stirred overnight. EtOAc (10 mL) was added to the reaction, and the solution was washed with $NaHCO_3$ (sat aq., 2 × 5 mL) and 10% citric acid (aq., 2 × 5 mL). The organic layer was dried (Na_2SO_4), filtered, and concentrated by rotary evaporation. The crude probes were then purified using preparatory C18 reversed-phase HPLC.

Probe 13 (CSIV.100A). The general procedure provided 5.7 mg (13%) of probe **13**. t_R(analytical): 15.1 min. ^{1}H NMR (500 MHz) δ 1.61−1.67 (m, 2H), 2.06 (td, *J* = 7.2, 2.6, 2H), 2.24 (td, *J* = 7.4, 2.6, 2H), 2.79−2.80 (m, 1H), 2.95−3.00 (m, 1H), 3.20 (dd, *J* = 13.7, 5.0, 1H), 4.43 (d, *J* = 6.1, 2H), 4.69−4.73 (m, 1H), 6.95 (br s, 1H), 7.07 (d, *J* = 7.8, 1H), 7.17 (t, *J* = 7.3, 1H), 7.07 (t, *J* = 8.2, 2H), 7.39 (d, *J* = 8.2, 2H), 7.51 (t, *J* = 7.5, 2H), 7.62 (t, *J* = 7.6, 2H), 7.72−7.77 (m, 5H), 7.91 (d, *J* = 8.3, 1H), 7.99 (d, *J* = 8.3, 1H), 8.32 (d, *J* = 8.5, 1H), 8.71 (t, *J* = 5.8, 1H), 9.97 (s,1H). ^{13}C NMR (125 MHz) δ 18.09, 25.12, 34.93, 38.53, 42.72, 54.62, 72.24, 84.94, 127.44, 127.58, 127.67, 127.68, 127.90, 128.70, 129.36, 129.39, 130.26, 130.30, 130.32, 130.47, 133.36, 133.56, 135.95, 138.14, 143.99, 144.298, 172.02, 172.41, 182.09, 196.35. HR-MS *m*/*z* calcd for $C_{36}H_{34}N_4O_4$ (M + H): 587.2653. Found: 587.2655.

Probe 14 (CSIV.100B). The general procedure provided 4.7 mg (11%) of probe **14**. t_R: 15.1 min. ^{1}H NMR (500 MHz) δ 1.62−1.66 (m, 2H), 2.06 (td, *J* = 7.2, 2.6, 2H), 2.24 (td, *J* = 7.4, 2.6, 2H), 2.95−3.00 (m, 1H), 3.20 (dd, *J* = 13.3, 5.2, 1H), 4.43 (d, *J* = 5.7, 2H), 4.69−4.73 (m, 1H), 6.86 (br s, 1H), 7.01 (d, *J* = 1.1, 1H), 7.11−7.15 (m, 1H), 7.29−7.39 (m, 3H), 7.50 (t, *J* = 8.1, 2H), 7.62 (t, *J* = 7.6, 2H), 7.72−7.77 (m, 5H), 7.91 (d, *J* = 8.3, 1H), 7.99 (d, *J* = 8.1, 1H), 8.31 (d, *J* = 8.5, 1H), 8.70 (t, *J* = 6.1, 1H), 9.88 (s, 1H). HR-MS *m*/*z* calcd for $C_{36}H_{34}N_4O_4$ (M + H): 587.2653. Found: 587.2653.

Probe 15 (CSIV.97). The general procedure provided 3.9 mg (16%) of probe **15**. t_R: 15.5 min. ^{1}H NMR (500 MHz) δ 1.64−1.68 (m, 2H), 2.07−2.11 (m, 2H), 2.24−2.28 (m, 2H), 2.79−2.82 (m, 1H), 2.95 (s, 1H), 3.02−3.09 (m, 1H), 3.20−3.25 (m, 1H), 4.82−4.86 (m, 1H), 6.73−6.76 (m, 1H), 6.90 (d, *J* = 8.3, 1H), 7.07 (m, 1H), 7.19 (m, 2H), 7.25−7.29 (m, 1H), 7.54−7.63 (m, 4H), 7.71−7.78 (m, 6H), 7.96 (d, *J* = 8.7, 1H), 8.01−8.04 (m, 1H), 8.45 (d, *J* = 8.0, 1H), 9.72 (s,1H), 10.46−10.51 (m, 1H). HR-MS *m*/*z* calcd for $C_{35}H_{32}N_4O_4$ (M + H): 573.2496. Found: 573.2490.

Probe 16 (CSIV.99). The general procedure provided 6.3 mg (16%) of probe **16**. t_R: 15.7 min. ^{1}H NMR (500 MHz) δ 1.64−1.69 (m, 2H), 2.07−2.12 (m, 2H), 2.24−2.18 (m, 2H), 2.79−2.82 (m, 1H), 2.95 (s, 1H), 3.02−3.09 (m, 1H), 3.20−3.25 (m, 1H), 4.82−4.86 (m, 1H), 6.91−6.93 (m, 1H), 7.05 (d, *J* = 7.4, 1H), 7.16 (td, *J* = 7.5, 1.0, 2H), 7.32 (d, *J* = 7.3, 1H), 7.54−7.63 (m, 4H), 7.71−7.80 (m, 7H), 7.96 (t, *J* = 8.8, 1H), 8.04 (d, *J* = 8.7, 1H), 8.46 (dd, *J* = 8.1, 2.6, 1H), 9.90 (s,-1H), 10.48−10.51 (m, 1H). ^{13}C NMR (125 MHz) δ 18.11, 25.14, 34.81, 38.51, 55.48, 72.29, 84.94, 119.38, 119.488, 127.60, 129.38, 129.403, 129.68, 129.68, 130.30, 130.35, 130.35, 130.45, 130.45, 133.40, 133.43, 136.09, 138.11, 142.61, 143.80, 171.44, 172.62, 196.38. HR-MS *m*/*z* calcd for $C_{35}H_{32}N_4O_4$ (M + H): 573.2496. Found: 573.2497.

Probe 19 (CSIV.101). Wang resin (200 mg, 0.220 mmol) was modified to display a resin bound *O*-hydroxylamine prepared as previously described.[14] A portion of the resin (60 mg) was added to a fritted syringe and swollen with CH_2Cl_2 (1 mL) for 1 h. A solution of Fmoc-aminohexanoic acid-OH (71 mg, 0.20 mmol), HATU (76 mg, 0.20 mmol), and *i*-Pr_2EtN (66 μL, 0.40 mmol) in DMF (0.5 mL) was added to the resin and agitated overnight. The resin was then filtered and washed with DMF (3 × 1 mL), the Fmoc group was removed (subjected to 20% piperidine in DMF for 30 min), and the resin was washed again (3 × 1 mL DMF). A solution of Fmoc-PABA-OH (72 mg, 0.20 mmol), HATU (76 mg, 0.20 mmol), and *i*-Pr_2EtN (66 μL, 0.40 mmol) in DMF (0.5 mL) was added to the resin and agitated for 4 h. The resin was then filtered and washed with DMF (3 × 1 mL), the Fmoc group was removed, and the resin was washed again (3 × 1 mL DMF). A solution of Fmoc-L-Bpa-OH (98 mg, 0.20 mmol), HATU (76 mg, 0.20 mmol), and *i*-Pr_2EtN (66 μL, 0.40 mmol) in DMF (0.5 mL) was added to the resin and agitated overnight. The resin was then filtered and washed with DMF (3 × 1 mL), the Fmoc group was removed, and the resin was washed again (3 × 1 mL DMF). A solution of 6-hexynoic acid (22 μL, 0.20 mmol), HATU (76 mg, 0.20 mmol), and *i*-Pr_2EtN (66 μL, 0.40 mmol) in DMF (0.5 mL) was added to the resin and agitated overnight. The acylation was repeated overnight, and the resin was then filtered and washed successively with DMF, THF, MeOH, THF, and CH_2Cl_2 (3 × 1 mL). The probe was cleaved from support by treatment with 97.5% TFA/2.5% H_2O, and the eluant was concentrated and then purified using preparatory C18 reversed-phase HPLC (t_R 14.2 min) to provide 5.6 mg (16%) of probe **19**. ^{1}H NMR (500 MHz) δ 1.32−1.35 (m, 2H), 1.55−1.67 (m, 6H), 2.00−2.11 (m, 4H), 2.25 (td, *J* = 7.3, 1.6, 2H), 2.80 (t, *J* = 2.6, 1H), 3.01−3.06 (m, 1H), 3.19−3.30 (m, 3H), 4.80−4.84 (m, 1H), 7.54−7.62 (m, 4H), 7.70−7.73 (m, 8H), 7.86 (d, *J* = 8.7, 1H), 8.37−8.43 (m,2H), 10.39 (s, 1H). ^{13}C NMR (125 MHz) δ 18.11, 25.14, 25.81, 27.02, 29.84, 33.13, 34.81, 38.51, 41.01, 55.43, 72.28, 84.93, 119.35, 128.84, 129.39, 130.28, 130.32, 130.34, 130.43, 133.40, 136.07, 138.11, 142.00, 143.83, 166.35, 169.94, 171.30, 172.58, 196.37. HR-MS *m*/*z* calcd for $C_{35}H_{38}N_4O_6$ (M + H): 611.2864. Found: 611.2856.

HDAC Activity Assay. HDAC activity was determined using a fluorogenic substrate assay kit (Fluor de Lys, Biomol, Plymouth Meeting, PA). In vitro assays were performed per manufacturer's instructions. HeLa nuclear lysate was diluted 1:30 with the provided assay buffer (50 mM Tris-HCl, pH 8.0, 137 mM NaCl, 2.7 mM KCl, 1 mM $MgCl_2$), and 15 μL were added to the well of a white 96 well plate. Inhibitors diluted in assay buffer (10 μL of 0−900 μM inhibitor, less than 10% DMSO) were added to nuclear lysate and preincubated for 15 min at rt. The assay was initiated by the addition of substrate (25 μL of 1.25 μM substrate in assay buffer). After 25 min at rt, the assay was quenched with the addition of 50 μL of developer (1:40 developer solution, 2 μM TSA in assay buffer). The fluorescence of the assay wells was detected at $\lambda_{ex}/\lambda_{em}$ 360/480 nm using a SPECTRAmax plate reader (Molecular Devices, Sunnyvale CA). IC_{50} values were determined by fitting the data from replicate trials (n = 2 or 3) to a sigmoidal dose−response curve using GraphPad Prism (GraphPad Software, San Diego, CA).

Cytotoxicity Assay. Cell viability assays were performed by distributing cells into the wells of a clear-bottomed 96-well plate (1000 cells/well). After 24 h, the media was replaced with media (100 μL/well) containing 0−60 μM parthenolide (or vehicle alone) and incubated for 4 h at 37 °C. After 4 h, WST-1 assay reagent (10 μL/well, Roche Applied Science) was added. After an additional incubation of 2.5 h, the absorbance of each well was detected at 420 nm using a SPECTRAmax plate reader (Molecular Devices, Sunnyvale CA). The background absorbance from 680 nm and from media + reagent alone was subtracted from the absorbance of each well, and the average corrected value from three independent trials was reported.

Results and Discussion

Optimization of Proteome Labeling Conditions for SAHA-BPyne. In the original experiments with SAHA-BPyne, we used a combination of gel- and mass-spectrometry-based approaches to identify multiple HDAC enzymes, including HDACs 1, 2, 3, and 6, as specific targets of this probe.[8] Furthermore, by virtue of the benzophenone moiety, SAHA-BPyne was also found to cross-link to and report on HDAC-associated proteins (e.g., CoREST, MBD3, and the metastasis associated proteins MTA1 and 2) bound proximally to the HDAC active site. While similar levels of HDAC complex components were found in many of the cell lines tested, some differences were observed. For example, HDAC6 labeling was observed in higher levels in the nonaggressive melanoma cell line, MUM2C, relative to its invasive counterpart, MUM2B. Conversely, the levels of CoREST in complex with HDACs were found to be higher in the aggressive MUM2B cell line. These results were validated using traditional western blotting methods, demonstrating that SAHA-BPyne can accurately measure differences in both HDAC content and complex assembly in native proteomes.

SAHA-BPyne was demonstrated to label HDAC complex proteins both in proteomes at 100 nM and in live cells at 500 nM, but we wondered whether we could achieve improved yields of protein labeling and a better depth of coverage by varying the probe concentration. To this end, we studied the effects of SAHA-BPyne concentration in the MUM2B cell line, where specific, HDAC-related labeling events were defined as those that could be blocked by the addition of excess SAHA (Figure 3). SAHA-BPyne was added to the soluble fraction of MUM2B proteome (1 mg/mL) at a concentration range of 50 nM−5 μM with or without excess SAHA (20×), crosslinked at 365 nm on ice, and treated with click chemistry reagents to append a rhodamine tag. The samples were separated by SDS-PAGE analysis and analyzed by in-gel fluorescence scanning. We observed increased signals for three specific targets, two at ∼60 kD (previously determined to be HDACs 1 and 2) and one at ∼30 kD (previously determined to be the HDAC-associated protein MBD3),[8] with increasing probe concentration; however, increased background labeling (not competed by SAHA) presented a problem, particularly at higher concentrations of probe (1−5 μM) (Figure 3A).

To determine if HDAC-enriched proteomic preparations might display decreased background, we compared the soluble proteome to the nuclear fraction of MUM2B cells (Figure 3B). Nuclear proteomes demonstrated improved sensitivity (higher signal intensities of SAHA-sensitive targets) and modest improvements in selectivity (decreased intensity of SAHA-insensitive bands, most notable around the molecular mass range of MBD3). We also observed one additional target, at ∼45 kD, that we had not observed in the soluble fraction. However, since some HDACs are not found in the nucleus,[1] we hoped that SAHA-BPyne might also be amenable to profiling in whole cell lysates, which encompass all proteomic fractions of the cell (soluble, nuclear, and membrane). Surprisingly, we observed improved selectivity for SAHA-sensitive targets in whole cell proteomes relative to either the simplified soluble or nuclear fractions, as well as maintenance of labeling of the 45 kD target (Figure 3C), indicating that SAHA-BPyne performed particularly well in proteomic samples of very high complexity.

Finally, we compared *in vitro* proteome reactions with labeling in live cells (*in situ*). SAHA-BPyne (50 nM−5 μM) was added, either alone or in the presence of excess SAHA (20×), to cultured preparations of MUM2B cells. The cells were then irradiated with UV light, washed (to remove excess probe), and homogenized. Treatment of the whole cell lysates with rhodamine-azide under click chemistry conditions and analysis by SDS-PAGE coupled with in-gel fluorescence scanning revealed a number of SAHA-sensitive targets (Figure 3D). Here, we observed clearly superior selectivity compared to *in vitro* labeling experiments, with low background even at the highest concentrations of probe tested, and were able to detect a fifth specific target of SAHA-BPyne at ∼125 kD. Similar results were found with the breast cancer cell line MDA-MB-231, with which we also observed improved sensitivity and selectivity of HDAC labeling profiles *in situ* relative to *in vitro* proteomic preparations (data not shown). These data collectively indicate that SAHA-BPyne is a versatile ABPP probe for HDAC complexes capable of functioning in a variety of proteomic fractions, including those as complicated as whole cell lysates, and remarkably shows its most robust behavior *in situ*.

Structure−Activity Relationship (SAR) for Labeling of HDAC Complexes by SAHA-BPyne and Related Probes. We next studied the SAR of SAHA-BPyne and examined if probes based on different scaffolds might exhibit enhanced labeling of specific targets. For these studies, we chose to maintain three key features of SAHA-BPyne: (1) the polar headgroup (conserved among all reported HDAC inhibitors and thought to interact with the active site metal cation),[15] (2) the benzophenone crosslinker (to provide irreversible labeling), and (3) the alkyne tag (to allow click chemistry-mediated conjugation to a rhodamine reporter tag), which, together, would allow us to assay the probes via the gel-based ABPP methods described above. We prepared a series of potential probes (Figure 2) that varied in (1) linker length (distance between polar headgroup and affinity group), (2) benzophenone position, and (3) the identity of the polar headgroup and other affinity elements.

The first analogue that we prepared possessed a shorter alkyl chain linker between the hydroxamate headgroup and benzophenone crosslinker than that for SAHA-BPyne, envisioning that such a change might allow for more optimal binding to HDACs with shallower active site pockets. Probe **6**, containing a glutaric acid linker (two methylenes shorter than SAHA-BPyne's suberic acid linker), was prepared in three steps from commercially available 4,4′-diaminobenzophenone (Figure 4A). Conversely, we also examined the impact of increasing the distance between the hydroxamate to the benzophenone, which we thought might allow us to cross-link to more distally located HDAC-associated proteins. Probes **7** and **8**, which share an identical linker as SAHA-BPyne, but place the crosslinking moiety at a farther distance were prepared by loading a primary amine onto a BAL-type linker via reductive amination, followed by acylation using standard Fmoc-based solid-phase peptide synthesis (SPPS) techniques (Figure 4B). Further elaboration of the structures by SPPS, followed by cleavage from the support, yielded the methyl ester analogues of the probes. The methyl esters were treated with hydroxylamine in solution to provide the desired hydroxamate probes. Additionally, probes **17** and **18**, which have

(15) Grozinger, C. M.; Schreiber, S. L. *Chem. Biol.* **2002**, *9*, 3−16.

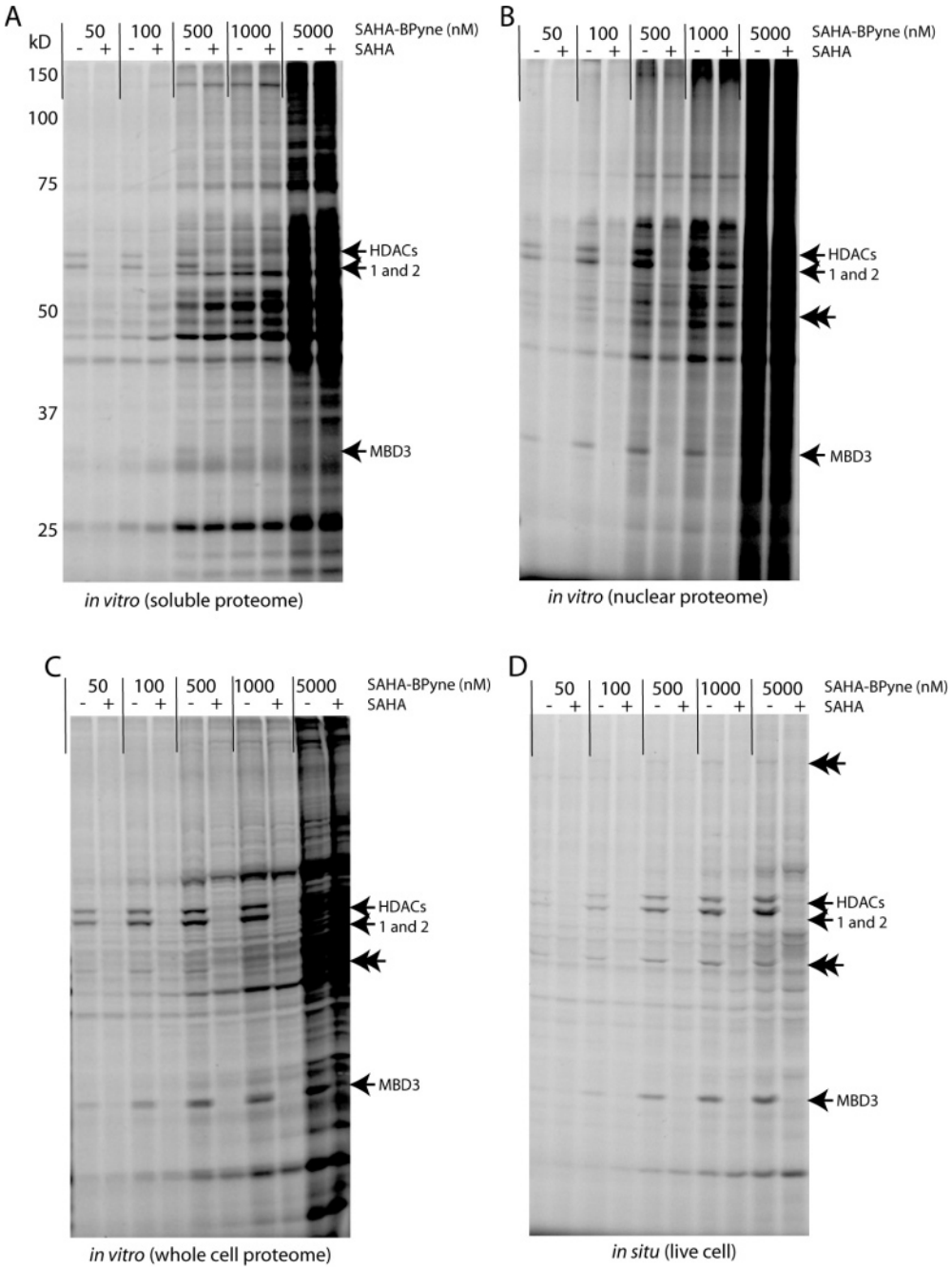

Figure 3. Comparison of proteome labeling by SAHA-BPyne over a probe concentration range of 50−5000 nM in soluble fractions (A), nuclear fractions (B), whole cell lysates (C), and *in situ* labeled cells (D). Gel lanes were loaded with 15 and 60 μg of protein for soluble/nuclear proteome and whole cell proteome/*in situ* labeling experiments, respectively. Specifically labeled targets of SAHA-BPyne were defined as proteins whose labeling was completed by excess SAHA (marked with arrowheads). Double arrowhead highlights additional specific targets of SAHA-BPyne that were detected with greater sensitivity in nuclear fractions (45 kDa), whole cell lysate (45 kD), and live cells (*in situ*) (45 and 125 kDa) relative to soluble fractions.

the same suberic acid linker as SAHA-BPyne, but modified affinity elements, were prepared by similar methods.

We next switched the linker from an alkyl chain to an aryl ring, a variation found in some previously reported HDAC inhibitors.[16,17] Probes **9**−**12** were prepared by modifying Wang resin to display a resin-bound *O*-hydroxylamine,[14] followed by standard Fmoc-based SPPS and cleavage from the solid support (Figure 4C). We also prepared probe **19**, an alkyl hydroxamate similar to SAHA-BPyne, but with a linker displaying a different pattern of H-bond donors and acceptors, by this method.

The final group of probes, **13**−**16**, was prepared with a benzamide polar headgroup, as found in the clinical candidates MS-275 (**3**) and CI-994 (**4**), instead of a hydroxamate. These probes were synthesized via addition of the first amino acid onto chlorotrityl resin, followed by standard Fmoc-based SPPS and cleavage from support to provide the corresponding carboxylic acid analogue of the probes. The benzamide was then installed by coupling to 1,2-phenylenediamine in solution (Figure 4D).

(16) Bouchain, G.; Delorme, D. *Curr. Med. Chem.* **2003**, *10*, 2359−72.
(17) Vannini, A.; Volpari, C.; Filocamo, G.; Casavola, E. C.; Brunetti, M.; Renzoni, D.; Chakravarty, P.; Paolini, C.; De Francesco, R.; Gallinari, P.; Steinkuhler, C.; Di, Marco, S. *Proc. Natl. Acad. Sci. U.S.A.* **2004**, *101*, 15064−9.

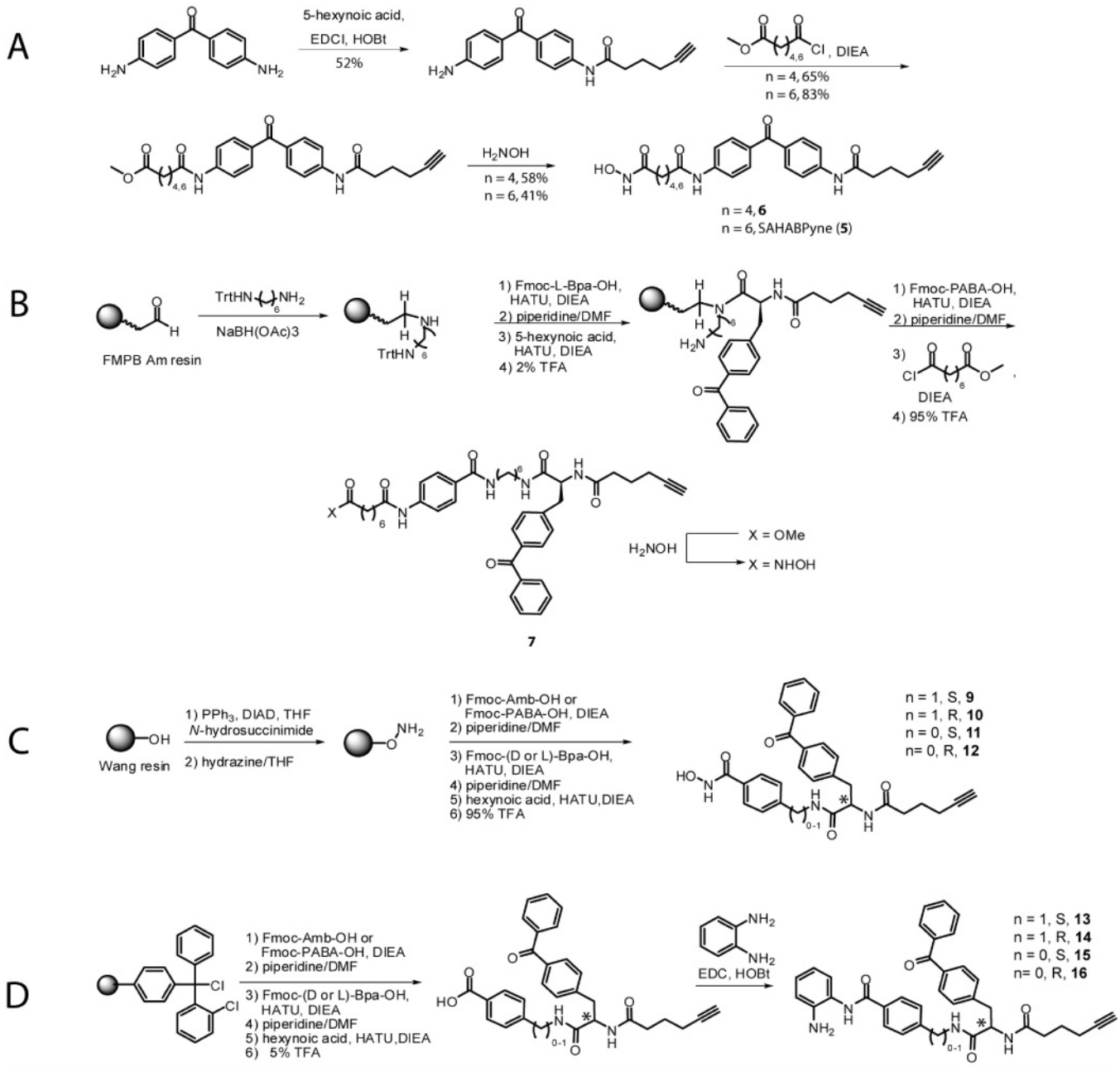

Figure 4. Synthesis of HDAC-directed ABPP probes. (A) Solution-phase synthesis of SAHA-BPyne and shorter linker length analogue **6**. (B) Preparation of **7**. Probes **8**, **17**, and **18** were prepared via a similar method, starting with reductive amination of 1-amino-5-hexyne onto FMPB AM resin. (C) Preparation of aryl hydroxamate probes. Probe **19** was prepared by coupling *N*-Fmoc-Ahx-OH onto *O*-hydroxylamine resin, followed by deprotection and elaboration via the steps shown. (D) Preparation of benzamide probes.

We tested the probes for specific HDAC labeling using both *in vitro* and *in situ* assays. First, we compared the labeling of protein targets in cytosolic and nuclear fractions of MUM2B cells as described above. Almost all of the hydroxamate probes performed adequately, showing labeling of HDACs 1 and 2 and MBD3 in the nuclear fraction (Figure 5A). Of the four aryl hydroxamate probes (**9**−**12**), the aminomethyl benzoic acid (Amb) derivatives (**9** and **10**) produced the most sensitive labeling of MBD3, whereas the highest signals for HDACs 1 and 2 were observed with *para*-aminobenzoic acid (PABA) derivatives (**11** and **12**). These findings suggest that the longer linker length of the Amb derivatives may allow the benzophenone moiety to extend further out of the HDAC pocket, thereby improving interactions with HDAC-associated proteins, whereas the benzophenone of the PABA derivatives interacts almost exclusively with the HDACs themselves. Of the two epimeric aryl hydroxamate PABA derivatives, higher intensity labeling was observed when the benzophenone amino acid input, 4-benzoyl-phenylalanine (Bpa), displayed an L conformation (compare compounds **17** versus **18**). These differences may reflect a lack of symmetry in the HDAC binding pockets, in either structure or sequence (benzophenones preferentially cross-link to Leu, Val, Lys, Arg, and Met residues[18]). In contrast to the hydroxamate probes, none of the four benzamide probes **13**−**16** showed any SAHA-sensitive targets (data not shown). The electronics of the benzophenone did not appear to dominate

(18) Dorman, G.; Prestwich, G. D. *Biochemistry* **1994**, *33*, 5661−73.

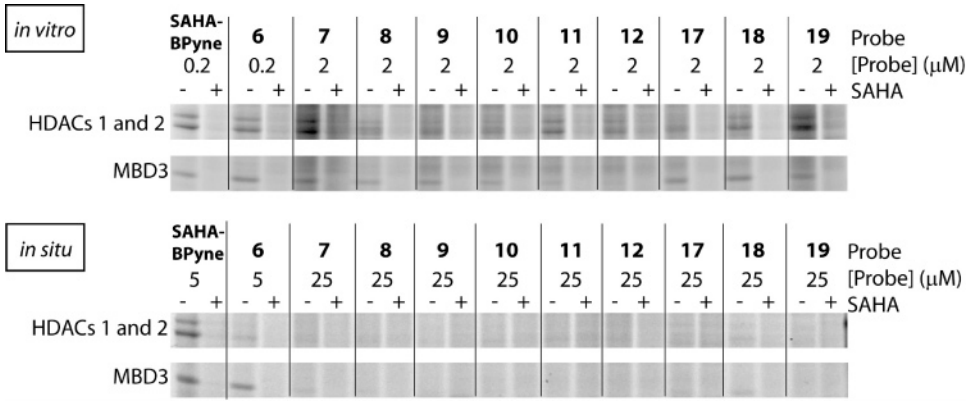

Figure 5. Comparison of *in vitro* (nuclear) versus *in situ* labeling profiles of HDAC-directed ABPP probes. Only relevant portions of the SDS-PAGE gels that contain HDACs 1 and 2 and MDB3 are shown.

the ability of the probes to photolabel HDAC complexes, as the probes with a weaker crosslinking potential[18] (probes **5** and **6**, containing electron donating substituents on the benzophenone) provided improved labeling over many of the other probes. Despite the diversity of structures, no new significant SAHA-sensitive targets were detected by gel analysis for any of the probes tested when compared to the profile of the original SAHA-BPyne probe.

We next tested all probes for *in situ* labeling of HDAC complexes in MUM2B cells, using SAHA-BPyne as a positive control. Surprisingly, none of the new sets of probes performed as well as SAHA-BPyne *in situ* (Figure 5B) even at concentrations up to 25 μM probe. At 5 μM, modest labeling of HDACs 1 and 2 and strong labeling of MBD3 were observed with probe **6**, the shorter linker length analogue of SAHA-BPyne. Probes **7**, **17**, and **18** also showed weak *in situ* labeling of MBD3 at 25 μM but no significant labeling of HDACs 1 or 2. These results demonstrate that *in vitro* labeling is not necessarily predictive of *in situ* labeling for ABPP probes.

Comparison of the Inhibitory Activities of Candidate HDAC-Directed ABPP Probes. To ascertain whether the differences observed in proteome labeling among the various probes were simply a reflection of their respective affinities for HDACs, we assessed the potency of probe binding by measuring inhibition of HDAC activity using a fluorogenic substrate assay kit (Figure 6). Overall, the hydroxamates were significantly more potent inhibitors of MUM2B HDAC activities than the benzamides, not a totally unexpected result, given that the benzamide analogues of some hydroxamate HDAC inhibitors show dramatically higher IC_{50} values (e.g., 3.5 μM vs 5 nM for trichostatin A).[16] This result suggests that the poor labeling of HDACs by benzamide-based probes may simply reflect weak binding interactions. Among the hydroxamate probes, no obvious correlation between IC_{50} values and HDAC labeling in proteomes was observed. Several probes inhibited HDAC activity more potently than SAHA-BPyne (e.g., probes **11** and **12**) but exhibited much weaker labeling of HDAC complexes in proteomes (Figure 5). This intriguing finding suggests that other factors, such as the location and orientation of the crosslinking moiety (and possibly the accessibility of the alkyne tag), are critical for converting a tight-binding reversible inhibitor into an optimal performing ABPP probe. On this note, benzophenones are capable of crosslinking to proteins within a range of $\sim$ 3.1 Å from the carbonyl bond,[18] and therefore, the location of the benzophenone (or other photocrosslinking groups) is likely an important consideration for the successful design of ABPP probes that operate by a photoreactive mechanism.

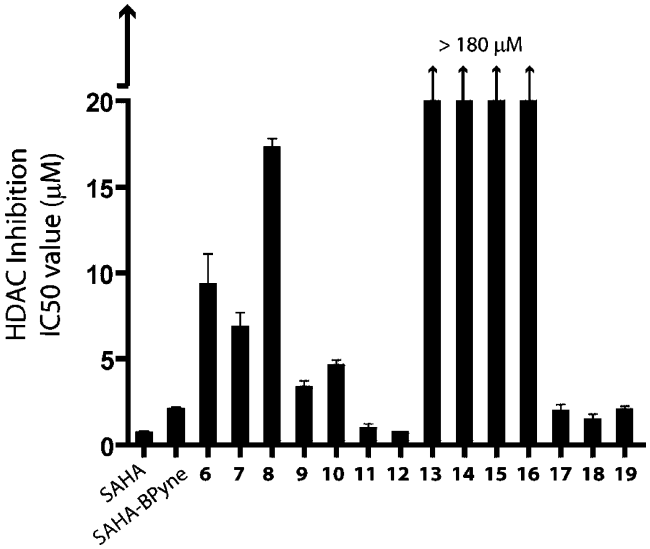

Figure 6. IC_{50} values for inhibition of HDAC activities in HeLa cell nuclear lysate by candidate ABPP probes. Results represent the average values $\pm$ standard errors for two-three independent experiments.

SAHA-BPyne allows for detection of changes in HDAC activity in live cells. The Van Dyke lab recently reported that the natural product parthenolide specifically depletes HDAC1 in a number of cell lines.[19] Using western blotting, the group was able to demonstrate that HDAC1 protein abundance decreases upon exposure to micromolar levels of parthenolide. To assess whether HDAC *activities* would be affected by parthenolide, we treated two human cancer cells lines, the colon cancer line HCT-15 and the breast cancer line MDB-MB-231, with 15 μM parthenolide for 3 h, followed by *in situ* analysis with SAHA-BPyne. SAHA-BPyne labeling confirmed that HDAC1 activity was decreased after parthenolide treatment in both cancer lines (Figure 7A and B). Attempts to induce a complete loss of HDAC1 signals by treating cancer cells with higher concentrations of parthenolide were thwarted by the marked toxicity displayed by this compound in HCT-15 cells (see below). Interestingly, in both cancer lines, parthenolide-treatment not only reduced HDAC1 activity but also produced

(19) Gopal, Y. N.; Arora, T. S.; Van, Dyke, M. W. *Chem. Biol.* **2007**, *14*, 813–23.

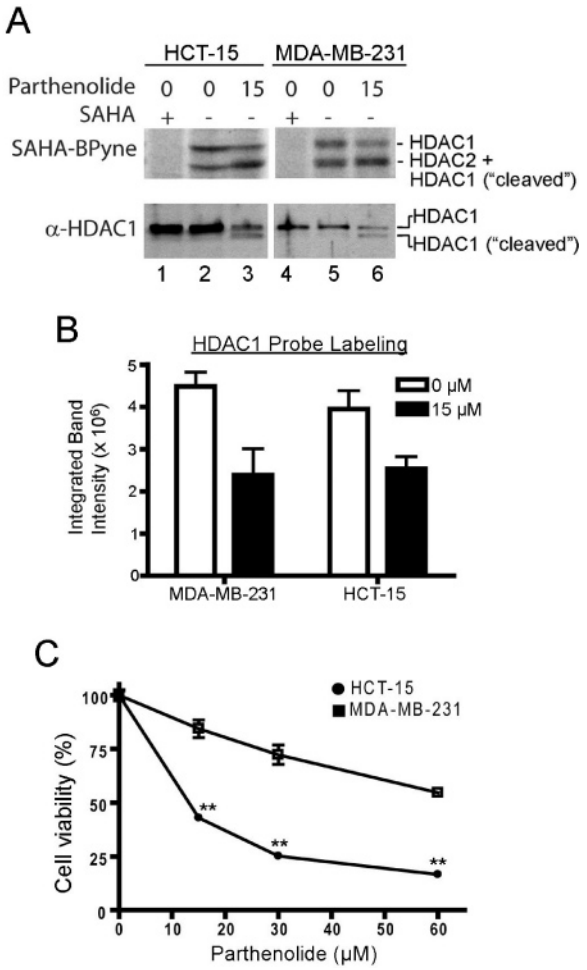

Figure 7. Parthenolide treatment of human cancer cell lines induces changes in HDAC1 activity and expression. (A) Effects of parthenolide on HDAC1 activity and protein levels, as judged by labeling with SAHA-BPyne (upper panels) and western blotting (lower panels), respectively. Note that parthenolide treatment induces the formation of a lower molecule mass, putatively "cleaved" form of HDAC1 that comigrates in the activity gel with HDAC2 (note that the slight differences in relative migration distance between the HDAC1 and HDAC1 "cleaved" signals on the activity gels and western blots are a result of running the samples on long and short SDS-PAGE gels, respectively). Gels and blots are representative examples of two to three independent experiments. (B) Quantification of the SAHA-BPyne labeling signals for HDAC1 in cancer cells treated with 0 or 15 μM parthenolide (treatment time of 3 h). Results are the average values $\pm$ standard errors for two to three independent experiments. (C) Cytotoxic effects of parthenolide in human cancer cell lines. Cancer lines were treated with parthenolide for 4 h, after which cell viability was measured as described in the Experimental Section. Results represent the average values $\pm$ standard errors for three independent experiments. $^{**}p < 0.01$, planned comparisons.

an increase in activity signals at a lower molecular mass that overlapped with HDAC2 (Figure 7A, upper panel). Western blotting revealed that, in addition to reducing HDAC1 protein levels in HCT-15 and MDB-MB-231 cells, parthenolide also induced the appearance of a lower molecular mass, putatively "cleaved" form of this protein that exhibited a similar molecular mass to HDAC2 (Figure 7A, lower panel; note that HDAC2 activity levels did not show any obvious changes following parthenolide treatment, consistent with previous findings indicating that this compound selectively reduces the levels of HDAC1[19]). To our knowledge, these results are the first demonstration that parthenolide can induce the formation of a lower molecular mass form of HDAC1 in cancer cells.

In the course of the aforementioned studies, we noted that HCT-15 cells appeared to exhibit much greater sensitivity to the cytotoxic effects of parthenolide compared to MDA-MB-231 cells. This premise was confirmed by evaluating the cytotoxic effects of parthenolide in these two cell lines. At all concentrations of parthenolide tested, HCT-15 cells showed a significantly greater cytotoxic response compared to MDA-MB-231 cells (Figure 7C). Curiously, however, HDAC1 activity signals were equal in intensity in these cell lines, as judged by SAHA-BPyne labeling (Figure 7A and B), indicating that the levels of HDAC1 in active histone-deacetylating complexes did not account for the observed differences in cell viablity. On the other hand, western blotting showed much greater total levels of HDAC1 protein in HCT-15 cells compared to MDA-MB-231 cells (Figure 7A, compare lanes 1 and 2 to lanes 4 and 5 in lower panels). These data thus suggest that, while the elevated sensitivity of certain cancer cells to parthenolide may be due to higher levels of HDAC1 expression, much of the excess HDAC1 does not appear to be engaged in active histone deacetylating complexes. The overexpression of HDAC1 in certain cancer cells may, hence, create a "free" pool of HDAC1 that possesses functions relevant to cell viability that extend beyond participation in protein complexes for histone deacetylation.

Conclusions

Here, we have investigated the proteome labeling profiles and inhibitory properties of SAHA-BPyne and related ABPP probes for HDACs. SAHA-BPyne, somewhat surprisingly, showed superior performance in terms of sensitivity and selectivity, when applied to the most complex biological systems, including whole cell lysates and living cells. One intriguing rationalization for this finding is that the maintenance of HDAC complexes in an optimally active form may require a variety of endogenous factors, some of which could be lost upon cell homogenization and/or fractionation. Given the diversity of post-translational mechanisms utilized by cells to regulate enzymatic pathways,[20] we expect that the optimal performance of many ABPP probes may be positively correlated with the integrity of biological samples under examination.

SAHA-BPyne further distinguished itself by effectively labeling HDAC complexes in live cells, whereas other probes tested targeted HDACs only *in vitro*. Interestingly, SAHA-BPyne does not appear to derive its value as an ABPP probe simply from enhanced potency in binding HDACs, as several probes showed stronger inhibitory activity in a substrate assay. Instead, other features of the SAHA-BPyne scaffold, including the location and accessibility of the benzophenone and alkyne moieties, are likely critical to efficiently translate binding into covalent labeling of HDAC complexes. Even these additional properties may not be sufficient to explain the unique capacity of SAHA-BPyne to label HDAC complexes in living cells. Here, we suspect that potential advantages of SAHA-BPyne may include enhanced cell permeability, distribution, and/or metabolic stability. Although these parameters are difficult to rationally design into small-molecule structures, they do suggest that constructing moderately sized probe libraries and testing these agents both *in vitro* and *in situ* may provide the most efficient route to optimized ABPP probes. Our results with

(20) Kobe, B.; Kemp, B. E. *Nature* **1999**, *402*, 373−6.

HDACs further argue that these probes do not need to be based on inhibitors of exceptional potency. Indeed, SAHA only displays a high nanomolar to low micromolar affinity for HDACs[1−3] but was still a suitable scaffold upon which to construct selective ABPP probes. Finally, by demonstrating that the levels of HDAC1 protein, but not necessarily activity, in cancer cells correlate with increased sensitivity to the cytotoxic agent parthenolide, we show how ABPP complements expression-based proteomic methods for discerning the impact of bioactive small-molecules on complex biological systems. We anticipate that the findings reported here, in addition to confirming the value of SAHA-BPyne as a reporter of HDAC activity and complex assembly in biological systems, may serve as a stimulus for the future development of additional classes of photoreactive, "clickable" ABPP probes for chemical proteomic endeavors.[21−23]

Acknowledgment. We acknowledge H. Hoover for technical assistance with cell culture and the Cravatt lab for their helpful discussions and suggestions. This work was supported by the American Cancer Society (PF-06-009-01-CDD, to C.M.S.), the National Institutes of Health (CA087660 and CA118696), and the Skaggs Institute for Chemical Biology.

JA074138U

(21) Ballell, L.; Alink, K. J.; Slijper, M.; Versluis, C.; Liskamp, R. M.; Pieters, R. J. *ChemBioChem* **2005**, *6*, 291−5.
(22) van Scherpenzeel, M.; van der Pot, M.; Arnusch, C. J.; Liskamp, R. M.; Pieters, R. J. *Bioorg. Med. Chem. Lett.* **2007**, *17*, 376−8.
(23) Sieber, S. A.; Niessen, S.; Hoover, H. S.; Cravatt, B. F. *Nat. Chem. Biol.* **2006**, *2*, 274−81.